Proceedings of the 40th IEEE
Conference on Decision and Control
Orlando, Florida USA, December 2001

Automatic Landing Control using H_∞ Control and Stable Inversion[1]

Jun Che[+]
Dept. of Flying Vehicle Design and Applied Mechanics
Beijing University of Aeronautics and Astronautics
Beijing, 100083, China

Degang Chen [*]
Dept. of Electrical and Computer Engineering
Iowa State University
Ames, IA 50011, USA

Abstract

This paper presents a new method for developing robust tracking controllers for automatic landing systems. We first develop a linearized longitudinal model of the Boeing 747 commercial airplane together with models for the control actuators, wind gust, and wind shear. The H_∞ control provides robust stability against uncertainties caused by exogenous disturbances and signals noise. The stable inversion provides precision tracking. Both methods are integrated to satisfy both robust and exact tracking requirements for the automatic landing system. Based on the stable inversion technique, the desired altitude and airspeed trajectories are also designed. The numerical simulation results show that the proposed automatic landing system can exceed FAA (Federal Aviation Administration) requirements for Category III precision approach landing. Furthermore, the integrated system can achieve robust accurate tracking in the presence of measurement noises, wind gust, and wind shear with middle intensity. Compared with existing approaches, our method achieved higher precision with excellent robustness.

1. Introduction

Today, most aircraft adopt flight control systems (FCS) to achieve good performance. The automatic landing system is one important function of modern flight control systems. Most conventional aircraft automatic landing systems use an instrument landing system (ILS) or a microwave landing system (MLS) in the terminal approach phase [1]. The kernel of the automatic landing system is the design of an automatic landing control law. As it is known, the most important performance requirements for passenger aircraft are safety and comfort. There are three phases in one flight: takeoff, cruise, and landing, with the landing phase the most challenging. During landing, the aircraft flies at a considerably low altitude, and hence accidents are more likely to happen. Many uncertain factors, such as wind gust, wind shear, also become critical because of low altitude and low speed. Measurement noise in the feedback signal is also stronger at ground level. Naturally, robustness to these uncertainties is a main challenge in the design of the automatic landing systems. On the other hand, during the landing, aircraft must track a desired trajectory satisfying FAA requirements until it arrives to the touchdown point in the runway. Therefore, the automatic landing control is inherently a tracking control problem.

There are many methods to design the automatic landing control law [2,3,4,5,6]. Shue and Agarwal [2] have developed a mixed H_2/H_∞ control technique for the design of an automatic landing system. Ochi and Kanai [4] adopted H_∞ control to design automatic approach and landing for propulsion controlled aircraft. But they did not treat the robustness of controller in the presence of wind shear, neither did they achieve accurate tracking performance. The neural network also was applied in the design of automatic landing system by Miller [5] and Saini [6]. However, the neural network approach is only effective within the special training set. A common weakness of these approaches is that they do not control the aircraft to track the desired flight path accurate. The purpose of this research is to design the automatic landing system control law by combining robust H_∞ control and stable inversion [7] to achieve both robustness and accurate tracking.

Landing Procedure: There are three phases in a typical landing procedure, initial approach, glide slope, and flare [8]. During the initial approach phase, the aircraft descends from cruising altitude to a lower altitude around 1500 feet. And then, the aircraft should enter altitude hold mode. It means that the aircraft keeps at a constant altitude and constant speed. Then, the aircraft enters a constant-descent or glide-slope mode, when the approach path intersects the desired glide path. During this phase, the aircraft should keep the flight path angle at -2.5 to -3 degrees, and maintain a constant speed. So, the sink rate of aircraft is $U_0 \sin\gamma$, where U_0 is aircraft velocity, and γ is the flight path angle. The transition maneuvers are designed to be safe and comfortable to passengers with accelerations not exceeding 0.15g. When the altitude of aircraft is equal to a special flare altitude h_{FLARE}, it enters the flare phase. The autopilot flies an asymptotic approach toward a final altitude h_F. In the touchdown point, the rate of descent must be reduced to less than about -2.0 feet/sec. During the glide slope phase, the transition maneuvers also need to satisfy the safe and comfortable requirement.

Requirement for Landing: Using the automatic landing system, the aircraft must be controlled in order to keep its path within a reference cone that guarantees the position and velocity accuracy required at touchdown. Table 1.1 shows FAA landing requirements[9].

Table 1.1 FAA navigation system accuracy standards

Operational phase	Minimum Altitude	Accuracy Lateral, 2 Drms	Vertical, Rms
En route terminal	152 m	7400 m	500 m
Approach landing			
Non-precision	76.2 m	3700 m	100 m
Precision Category I	30.5 m	9.1 m	3.0 m
Precision Category II	15.2 m	4.6 m	1.4 m
Precision Category III	0 m	4.1 m	0.5 m

The rest of the paper is organized as follows. An aircraft model is presented in section 2, together with models for the control actuators, wind gust, wind shear, and measurement noise. In section 3, the H_∞ optimal control design and the stable inversion design is described. Meanwhile, the desired trajectory is also designed in this section. In section 4, the results of the simulations are presented. The advantages of the new scheme are pointed out. Finally section 5 gives a brief summary and some conclusion.

[1]This work is supported in part by Rockwell Collins and by the National Science Foundation.

[+]Research Assistant, Work was performed while the author was at Iowa State University, e-mail: junche@iastate.edu
[*]Associate Professor, e-mail: djchen@iastate.edu

2. Aircraft Model

2.1 Longitudinal Linear Model of Airplane

In general, the standard six degrees of freedom (6DOF) equations of motion used for conventional aircraft control design and flight simulation can be obtained by the assumptions of the flat-Earth and rigid-body aircraft with longitude symmetric plane. In this paper, only the longitudinal motion was considered.

Using the small perturbation assumption from the steady-state condition, we can derive a set of linear constant-coefficient state equations. Usually, we call this steady-state as the equilibrium point. In this study, the aircraft is modeled in small perturbations around a stable equilibrium point. The particular steady-state equilibrium point is the landing configuration at sea level for a Boeing 747. In the presence of wind disturbances, a linear state-space model describing the aircraft longitudinal dynamics is given by [10]:

$$\dot{x} = Ax + Bu + B_w u_w \tag{2.1}$$

The state vector and input vector are:

$$x = [u, w, q, \theta, h]'$$

$$u = [\delta_e, \delta_t]'$$

$$u_w = [W_u, W_w]'$$

where, u = longitudinal ground speed, w = vertical ground speed, q = pitch rate, θ = pitch attitude angle, h = altitude, δ_e = elevator deflection, δ_t = commanded thrust force, W_u = x-axis wind velocity, and W_w = z-axis wind velocity.

Two additional variables that are commonly used are the air speed of aircraft V, and angle of attack (AOA) α. They are related to the state variables by the following:

$$V = \sqrt{u^2 + w^2} \tag{2.2}$$

$$\alpha = \tan^{-1}(w/u) \tag{2.3}$$

For $w^2 << u^2$, the relations are well approximated as:

$$V \cong u \tag{2.4}$$

$$\alpha \cong w/u \tag{2.5}$$

The pitch angle θ, angle of attack α, and flight path angle γ are related by:

$$\theta = \alpha + \gamma \tag{2.6}$$

Using aerodynamic derivatives, the A, B, B_w matrices can be obtained with numerical values (in units of feet, seconds, and centiradians) as follows [10]:

$$A = \begin{bmatrix} -0.0210 & 0.1220 & 0.0000 & -0.3220 & 0.0000 \\ -0.2090 & -0.5300 & 2.2100 & 0.0000 & 0.0000 \\ 0.0170 & -0.1640 & -0.4120 & 0.0000 & 0.0000 \\ 0.0000 & 0.0000 & 1.0000 & 0.0000 & 0.0000 \\ 0.0000 & -1.0000 & 0.0000 & 2.2100 & 0.0000 \end{bmatrix}$$

$$B = \begin{bmatrix} 0.0100 & 1.0000 \\ -0.0640 & -0.0440 \\ -0.3780 & 0.5440 \\ 0.0000 & 0.0000 \\ 0.0000 & 0.0000 \end{bmatrix}, \quad B_w = \begin{bmatrix} 0.0210 & -0.1220 \\ 0.2090 & 0.5300 \\ -0.0170 & 0.1640 \\ 0.0000 & 0.0000 \\ 0.0000 & 0.0000 \end{bmatrix}$$

Table 2.1 shows the open-loop system eigenvalues, damping ratio and frequency.

Table 2.1 Open-loop system characteristics

Mode	Eigenvalue	Damping ζ	Freq. (rad/s) ω_n
short-period	-0.4804± j0.6083	0.62	0.775
phugoid	-0.0011±j0.1523	0.00711	0.152

2.2 Elevator Actuator and Throttle Control Model

Usually, elevator and throttle can be represented using a first-order lag process. In this case, 0.1-s and 4-s time constants are selected for the elevator actuator and the throttle control model respectively[8].

2.3 Wind Disturbance Model

Turbulence is a stochastic process that can be defined by velocity spectra. In general, we can use zero mean white noise feeding through a shaping filter to simulate it. Usually, the shaping filter is chosen as a first-order dynamics for forward and vertical speed directions in this case [10]. Table 2.2 presents the correlation times used for each wind gust component [8]. In general, the value of τ depends on parameters of the airplane. It is different in different body axis, and at different trim point.

Table 2.2 Wind gust disturbance correlation times

Disturbance	τ (s^{-1})
Longitudinal wind	0.43
Vertical wind	1.06

2.4 Wind Shear Model

The wind shear model is a two dimensional model. Along the trajectory, the airplane will be faced with a headwind going up to about W_x = -12 ft/s, then wind speed will change to a tailwind of about W_x =12 ft/s, combined with a down draught of about W_h = 12 ft/s. The result of this will be a drastic decrease in aircraft energy. The aircraft will not be able to stay on the desired trajectory. The horizontal and vertical speed of the wind shear is given by [11]

$$W_x = -W_{x0} \sin\left(\frac{2\pi}{T_0}\right) \tag{2.7}$$

$$W_h = -W_{h0}\left[1 - \cos\left(\frac{2\pi}{T_0}\right)\right] \tag{2.8}$$

where T_0 is the total flight time through the wind shear. We choose

$$T_0 = 60(s), W_{x0} = 12(ft/s), W_{h0} = 6(ft/s)$$

2.5 Sensor and Measurement Noise Model

Models are not provided for the characteristics of the sensors: they are all assumed to be unity gain with additive noise. The measurement noises were simulated by zero-mean white noise with the corresponding standard deviation value.

3. Automatic Landing Control with H_∞ Control and Stable Inversion

3.1 H_∞ Controller Design

H_∞ control is a robust control method that optimizes the system performance, and achieves robust stability for an uncertain plant [12]. The principle design and analysis tools used for this design include the H_∞ synthesis functions of MATLAB μ-Synthesis

toolbox. These tools use a state-space representation of the linearized plant to determine an optimal or suboptimal H_∞ controller.

In our case, h and u are the variables we must control to follow the desired trajectory. And we select y, the feedback signals, as following [13]:

$$y = [h, \dot{h}, u, \dot{u}, \theta, q]$$

The basic architecture of the longitudinal controller is shown in Figure 3.1. This system uses the elevator deflection (δ_e) and the throttle position (δ_t) to control longitudinal aircraft dynamics. The input to the controller K, consists of attitude angle θ, pitch rate q (providing for inner-loop bandwidth and short period damping respectively) and errors in airspeed and altitude and the rates thereof. The main performance objective we address here is decoupled tracking of speed and altitude references (r = [h_{ref} ; u_{ref}]^T).

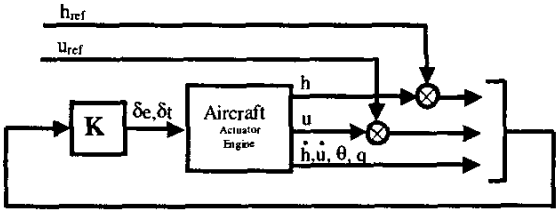

Figure 3.1. Controller architecture

According to the design specifications, our design must satisfy the performance, safety, actuator effort, and comfort requirement. In the conventional design procedure, the design objective is achieved through adjusting the controller gains. In the H_∞ control design procedure, the most important task is to select the weights based on the specifications.

In order to normalize the reference inputs, we should scale the altitude and speed commands. So, we select h_{max} and u_{max} as the weight W_{in}. Measurements will always be corrupted with some noise. W_n is the measurement noise weights. Meanwhile, we use the wind gust model as the weights of wind channels (W_w). Up to frequencies beyond the bandwidth of the ideal model filters, the differences between the altitude and speed responses and h_{ref} and u_{ref} respectively should be small. This requirement is reflected by the weight W_p. Note that weighting contains approximate double integration. We know that the controller at lower frequencies will have approximately the same shape. This enables the controlled system to track ramp commands with a very small steady state error. Weighting W_{pq} is applied in order to keep control over the pitch rate. Good tracking of the feed forward filter outputs should not be at the cost of extreme pitch rates. Weighting W_{act} is applied to constrain the controls and control rates. We use the values of the maximum deflections and rates.

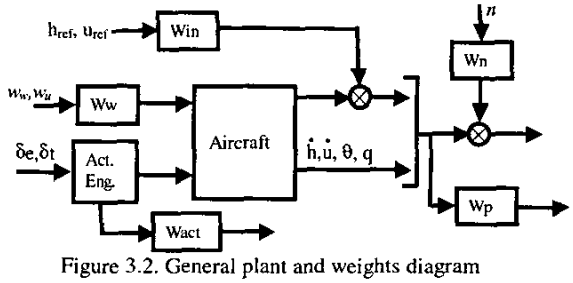

Figure 3.2. General plant and weights diagram

Based on above weights, we can obtain the controller using H_∞ design functions in the MATLAB μ-Synthesis toolbox. The achieved γ value is 0.4662. The order of the controller is 15. Eigenvalues of the closed loop system are negative, so it is stable.

Figure 3.3 is the frequency response of the closed loop system. Both altitude and speed loops achieved the same bandwidth. The diagonal plots in figure 3.4 reflect the achieved altitude and speed command response. It also shows that the two loops are decoupled. From these frequency plots, we can see the design requirements are met.

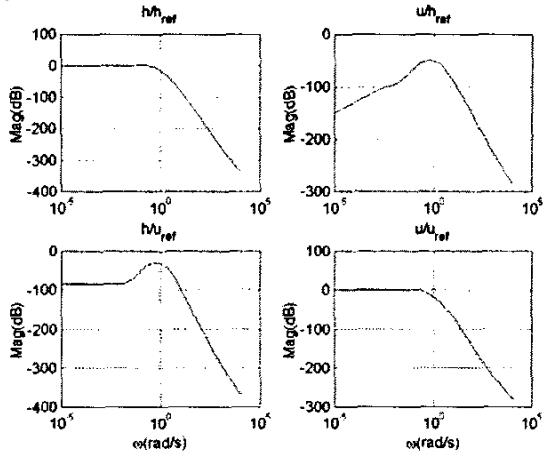

Figure 3.3. Frequency response of closed loop system

3.2 Stable Inversion Design

In this section, we describe the stable inversion theory. We consider the multivariable nonlinear system

$$\dot{x} = f(x) + g(x)u$$
$$y = h(x) \qquad (3.1)$$

where state $x \in \mathbf{R}^n$, output $y \in \mathbf{R}^p$, and input $u \in \mathbf{R}^p$. Assume that $f(0)=0$ and $h(0)=0$. For such a system, Chen has stated the stable inversion problem as follow [14]:

Stable Inversion Problem: Given a smooth reference output trajectory $y_d(t)$ with compact support, find a control input $u_d(t)$ and a state trajectory $x_d(t)$ such that

1) $u_d(t)$ and $x_d(t)$ satisfy the differential equation

$$\dot{x}_d = f(x_d(t)) + g(x_d(t))u_d(t);$$

2) exact output tracking is achieved

$$h(x_d(t)) = y_d(t);$$

3) $u_d(t)$ and $x_d(t)$ are bounded and

$$u_d(t) \to 0, \; x_d(t) \to 0 \text{ as } t \to \pm\infty.$$

In this paper, we only consider a linear system described by [7]

$$\dot{x}(t) = Ax(t) + Bu(t)$$
$$y(t) = Cx(t) \qquad (3.2)$$
$$z(t) = C_m x(t)$$

where $z(t)$ is the measurement output. If we set $y_d(t)$ as the desired output trajectory to be tracked, the nominal input and state trajectory $[u_d(t), \; x_d(t)]$ should be found to satisfy the equation (3.2), i.e.,

$$\left.\begin{aligned}\dot{x}_d(t) &= Ax_d(t) + Bu_d(t)\\ y_d(t) &= Cx_d(t)\\ z_d(t) &= C_m x_d(t)\end{aligned}\right\} \quad \forall t \in (-\infty,\infty) \qquad (3.3)$$

Then, we can use the feedback controller to stabilize the exact output yielding trajectory z_d. Thus we can obtain output tracking.

The key point is to find the inverse input-state trajectory $[u_d(t), x_d(t)]$. We use a change of coordinates T such that $[\xi(t),\eta(t)]' = Tx(t)$ where $\xi(t)$ consists of the output and its time-derivatives

$$\xi(t) \equiv \left[y_1, \dot{y}_1, \cdots, \frac{d^{r_1-1}y_1}{dt^{r_1-1}}, y_2, \dot{y}_2, \cdots, \frac{d^{r_2-1}y_2}{dt^{r_2-1}}, \cdots, y_p, \dot{y}_p, \cdots, \frac{d^{r_p-1}y_p}{dt^{r_p-1}} \right]'.$$

Where, $r := [r_1, r_2, \ldots, r_p]$ is vector relative degree. Now, we rewrite the system equation (3.2) in the new coordinates as

$$\dot{\xi}(t) = \hat{A}_1\xi + \hat{A}_2\eta + \hat{B}_1 u \qquad (3.4)$$

$$\dot{\eta}(t) = \hat{A}_3\xi + \hat{A}_4\eta + \hat{B}_2 u \qquad (3.5)$$

where

$$\hat{A} = TAT^{-1} = \begin{bmatrix}\hat{A}_1 & \hat{A}_2\\ \hat{A}_3 & \hat{A}_4\end{bmatrix};\ \hat{B} = TB = \begin{bmatrix}\hat{B}_1\\ \hat{B}_2\end{bmatrix}.$$

Note that the desired ξ is known when the desired output trajectory y_d and its time derivatives are specified. This desired ξ is defined as ξ_d. Since the control law is chosen such that exact tracking is maintained, $y^{(r)}(t) = y_d^{(r)}(t)$, we also have $\dot{\xi}(t) = \dot{\xi}_d(t)$, and equations (3.4) and (3.5) become

$$\dot{\xi}(t) = \dot{\xi}_d(t) \qquad (3.6)$$

$$\dot{\eta}(t) = \hat{A}_3\xi_d(t) + \hat{A}_4\eta(t) + \hat{B}_2 B_y^{-1}[y_d^{(r)}(t) - A_\xi\xi_d(t) - A_\eta\eta(t)] \qquad (3.7)$$

Rewrite equation (3.7) as

$$\dot{\eta}(t) = \hat{A}_\eta\eta(t) + \hat{B}_\eta Y_d(t) \qquad (3.8)$$

where $Y_d(t) \equiv [y_d^r(t), \xi_d(t)]'$.

This is the inverse system. If we can find a bounded solution, η_d, to the dynamics (3.8), then the desired feed forward input can be found as

$$u_d(t) = B_y^{-1}[y_d^{(r)}(t) - A_\xi\xi_d(t) - A_\eta\eta_d(t)] \qquad (3.9)$$

and the desired state trajectory will be

$$x_d(t) = T^{-1}\begin{bmatrix}\xi_d\\ \eta_d\end{bmatrix}.$$

So the desired measurement output is

$$z_d(t) = C_m x_d(t) = C_m T^{-1}\begin{bmatrix}\xi_d\\ \eta_d\end{bmatrix}.$$

Now, we use the stable inversion technique to design a control law for our Boeing 747 airplane. We assume the desired trajectory is $y_d(t) = [h_d, U_d]$. Altitude (h) and forward speed (U) are the variables we must control to follow the desired trajectory. And $z(t)$ is used as the feedback signal. Then, we can use the stable inversion theory to design feed forward input u_d and reference output z_d. Note that this system includes the elevator's actuator and engine dynamics. So, the state $x = [\delta_e, \delta_t, U, w, q, \theta, h]'$, input $u = [\delta_{ec}, \delta_{tc}]'$, output $y = [h, U]'$, and measurement output $z = [h, \dot{h}, U, \dot{U}, \theta, q]$.

It is not difficult to show that the system have well defined relative degree, $r = [r_1, r_2] = [3,2]$. According to the change of coordinates, ξ is defined as $\xi(t) = [h, \dot{h}, \ddot{h}, U, \dot{U}]$. Then, we can obtain the transformation T let

$$\begin{bmatrix}\xi(t)\\ \eta(t)\end{bmatrix} = Tx(t)$$

$$= \begin{bmatrix} 0 & 0 & 0 & 0 & 0 & 0 & 1.0000\\ 0 & 0 & 0 & -1.0000 & 0 & 2.2100 & 0\\ 0.0640 & 0.0440 & 0.2090 & 0.5300 & 0 & 0 & 0\\ 0 & 0 & 1.0000 & 0 & 0 & 0 & 0\\ 0.0100 & 1.0000 & -0.0210 & 0.1220 & 0 & -0.3220 & 0\\ 0 & 0 & 0 & 0 & 1.0000 & 0 & 0\\ 0 & 0 & 0 & 0 & 0 & 1.0000 & 0 \end{bmatrix} x(t)$$

By using equation (3.9) the inverse input can be written as

$$u_d(t) = \begin{bmatrix} 1.5733 & -0.0692\\ -0.6293 & 4.0277\end{bmatrix}\left\{\begin{bmatrix}\ddot{h}_d\\ \ddot{U}_d\end{bmatrix} - \begin{bmatrix} 1.1713 & 11.8147\\ -0.0524 & 1.7872\end{bmatrix}\eta(t) - \begin{bmatrix} 0 & -5.2831 & -10.5975 & 2.1132 & 0.6410\\ 0 & -0.8353 & -1.6560 & 0.3168 & -0.2035\end{bmatrix}\xi_d(t)\right\} \qquad (3.10)$$

From equation (3.8), we can obtain

$$\dot{\eta}(t) = \begin{bmatrix} -0.4120 & 6.7461\\ 1.0000 & 0\end{bmatrix}\eta(t) + \begin{bmatrix} 0 & 0 & 0 & -2.9346 & -6.0327 & 1.2948 & 0.8094\\ 0 & 0 & 0 & 0 & 0 & 0 & 0\end{bmatrix} Y_d(t) \qquad (3.11)$$

where $Y_d = [\dddot{h}_d, \ddot{U}_d, h_d, \dot{h}_d, \ddot{h}_d, U_d, \dot{U}_d]'$.

The problem is to find the bounded solution to equation (3.11). We can use a transformation V to decouple the system into a stable subsystem (σ_s) and an unstable subsystem (σ_u):

$$\dot{\sigma}_s(t) = [-2.8115]\sigma_s(t) + [0\ \ 0\ \ 0\ \ 1.6805\ \ 3.4546\ \ -0.7415\ \ -0.4635]Y_d(t) \qquad (3.12)$$

$$\dot{\sigma}_u(t) = [2.3995]\sigma_u(t) + [0\ \ 0\ \ 0\ \ 1.4639\ \ 3.0095\ \ -0.6459\ \ -0.4038]Y_d(t) \qquad (3.13)$$

where

$$\sigma(t) = \begin{bmatrix}\sigma_s(t)\\ \sigma_u(t)\end{bmatrix} = V\eta(t) = \begin{bmatrix} -0.9422 & -0.9230\\ 0.3351 & -0.3847\end{bmatrix}\eta(t).$$

The stable subsystem is integrated forward in time and the unstable subsystem is integrated backward in time to guarantee boundedness. We can get then the bounded solution, η_d. Finally, we can use equation (3.11) to obtain feed forward input u_d and desired measurement output z_d.

3.3 Integration of H_∞ Control and Stable Inversion

Figure 3.4 shows how to integrate the stable inversion and H_∞ controller. This integrated approach can satisfy both robust and exact tracking requirements. Note that the calculation of stable inversion is off-line based on the desired landing trajectory. Usually, in the landing process, this trajectory is known. So, when an aircraft arrives at the airport, the flight computer can calculate an ideal trajectory according to its position and speed. H_∞ controller uses the errors between the desired and the actual measurement signals as the feedback variables. The controller calculates the feedback control input on-line for airplane, and adds the desired control input u_d to drive the airplane motion. The

remaining task is to design a desired trajectory for the airplane landing process.

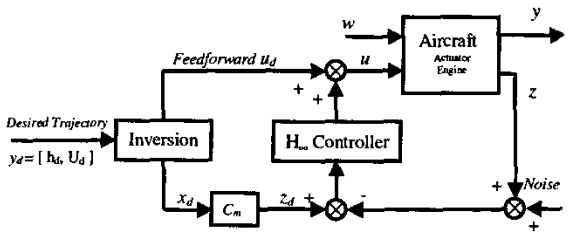

Figure 3.4. Block diagram of stable inversion and H_∞ control

3.4 Desired Landing Trajectory Design

In this subsection, we will discuss the design of the desired trajectory for airplane landing. We have two variables that are controlled to follow the desired trajectory. One is the forward speed U; and another one is the altitude h. According to the landing requirements, the aircraft descends from cruising altitude to a lower altitude around 1500 feet. Meanwhile, the speed of the aircraft also reduces from the cruising speed to an approach speed, and keeps it as a constant. So, when we design the desired trajectory, we design the desired forward speed U first. Then we design the desired altitude trajectory. The altitude trajectory design includes two parts: level flight to the glide slope design, and glide slope to flare design. The principle idea is to keep the second-order derivative of U continuous, and the third-order derivative of h will be kept continuous too.

4. Simulation Results

4.1 Numerical Simulation Set up

In this section, using the methods and parameters described in the previous sections, we simulate the automatic landing system. Note that the Boeing 747 airplane model is based on altitude at sea level and airspeed of 221 ft/s. The steady equilibrium attitude is 8 deg. The initial approach altitude is 1500 feet, glide-slope angle is 3 deg, flare path phase begins at 92 feet altitude, altitude of aircraft C.G. is 12 feet at touchdown, and the sink rate at touchdown point is –0.5 feet/sec.

In this research, MATLAB 5.3 based on MS windows 98 is employed. We use the H_∞ synthesis functions of MATLAB μ-Synthesis toolbox to design the H_∞ controller. SIMULANK is used to simulate the whole landing process.

4.2 Results and Discussion

In this case, the airplane begins at a speed initially exceeding the normal airspeed by 10 ft/s. This speed should be reduced to the normal speed 221 ft/s and then kept at this value. This landing process begins at a 1500 feet altitude. Actually, there exist the measurement noise of sensors and wind gust when an airplane lands in the airport. As we know, low-altitude wind shear has been recognized as a serious threat to the safety of aircraft in landing. The problem of guiding an aircraft encountering wind shear has received considerable attention. We assume that the airplane meets a wind shear with low intensity in the glide slope phase. Figure 4.1-4.6 show the simulation results based on this case. Figure 4.1 shows that the airplane also tracks the desired trajectory well, even under the wind shear condition. From Figure 4.2, we can see that the largest error between the desired path and the actual path is less than 5 ft when the airplane is within the wind shear, and it is 0.3 ft at touchdown point. The sink rate and forward speed are shown in Figure 4.3 and 4.4. Figure 4.5 shows that the largest errors of sink rate and forward speed are 0.9 ft/s and 1.8 ft/s respectively. The error of sink rate is 0.1ft/s at touchdown point. In the glide slope phase, flight path angle is also around –3 deg, and its error is about 0.25 deg (Figure 4.6).

It meets the FAA Category III accuracy requirement in Table 1.1. The reason that our design meets the requirement and achieves the design goal is that we adopt the H_∞ robust control technique. H_∞ controller can handle the plant with measurement noise of sensors and wind gust. This case also shows that the design could reject a wind shear with such intensity. Usually, this kind of rejection role is limited because most wind shear has more energy. If wind shear is strong, a pilot's strategy is often to avoid having the aircraft enter into wind shear.

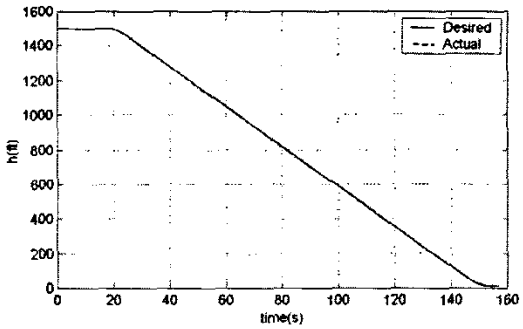

Figure 4.1. Altitude of airplane in landing

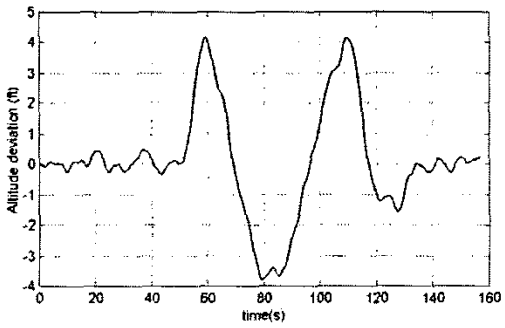

Figure 4.2. Altitude deviation in landing

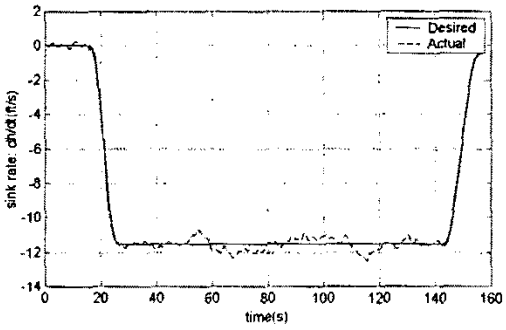

Figure 4.3. Sink rate of airplane in landing

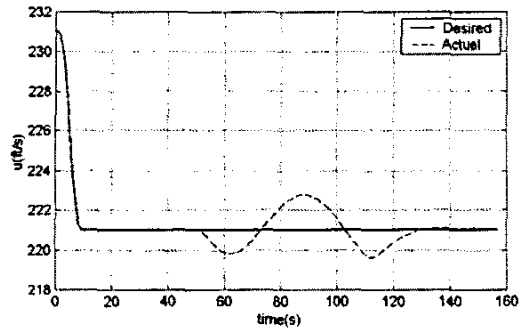

Figure 4.4. Forward speed of airplane in landing

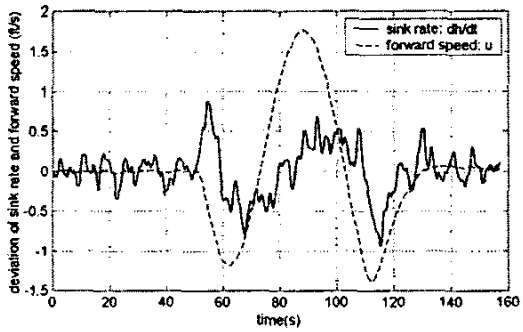

Figure 4.5. Sink rate and forward speed deviation

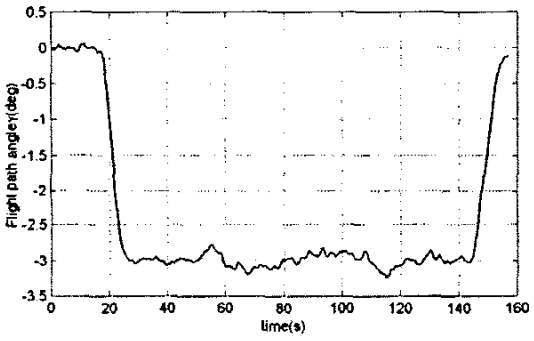

Figure 4.6. Flight path angle of airplane in landing

5. Conclusion

A new method combining H_∞ robust control and stable inversion has been formulated for the design of automatic landing systems. This method can handle both robustness and exact tracking problem, and thus is very well suited for the design of automatic landing system. The method was successfully tested with a Boeing 747 commercial airplane model together with control actuator, wind gust, and wind shear models.

Simulation results demonstrate that by using stable inversion and H_∞ control, the aircraft could track the desired trajectory very accurately. The control law has the ability to reject the measurement noise from sensors, wind gust, and wind shear with low intensity. The automatic landing system can meet FAA requirements for Category III approach landing. Clearly, this system also satisfies the stability and robustness requirement. Furthermore, the reference airspeeds and landing angles for the landing system are within the FAA standards. Compared with existing approaches in automatic landing system, our method achieved much higher tracking precision.

In this research, we only used a linearized model to verify the proposed method. Future work is needed for simulation study with a nonlinear airplane model to determine the applicability of our method, which is based on the linear plant, to the nonlinear plant. To further improve our method, design of H_∞ controller can be based on the linear plant, while the stable inversion design can be done using the nonlinear plant. Furthermore, intelligent control and learning control could be incorporated to augment the system's decision and tolerating ability.

References

[1] Galotti, V. P., *The Future Air Navigation System (FANS)*, Avebury, Aldershot, England, 1997.

[2] Shue, S., and Agarwal, R. K., "Design of Automatic Landing Systems Using Mixed H_2/H_∞ Control," *Journal of Guidance, Control, and Dynamics*, Vol. 22, No. 1, 1999, pp. 103-114.

[3] Niewoehner, R. J., and Kaminer, I. I., "Design of an AutoLand Controller for Carrier-Based F-14 Aircraft using H_∞ Output-Feedback Synthesis," *Proceeding of the American Control Conference*, Baltlmore, Maryland, June 1994, pp. 2501-2505.

[4] Ochi, Y., and Kanai, K., "Automatic Approach and Landing for Propulsion Controlled Aircraft by H_∞ Control," *Proceedings of the 1999 IEEE International Conference on Control Applications*, Kohala Coast-Island of Hawaii, Hawaii, August 1999, pp. 997-1002.

[5] Miller, W. T., III, Sutton, R. S., and Werbos, P. J., *Neural Networks for Control*, Bradford Book, MIT Press, Cambridge, MA, 1992, pp. 403-426.

[6] Saini, G., and Balakrishnan, S. N., "Adaptive Critic Based Neurocontroller for Autolanding of Aircraft," *Proceedings of the American Control Conference*, Albuquerque, New Mexico, June 1997, pp. 1081-1085.

[7] Devasia, S., "Output Tracking with Nonhyperbolic and Near Nonhuperbolic Internal Dynamics: Helicopter Hover Control," *Proceedings of the American Control Conference*, Albuquerque, New Mexico, June 1997, pp. 1439-1446.

[8] Parkinson, B. W., O'Connor, M. L., and Fitzgibbon, K. T., "Aircraft Aotumatic Approach and Landing Using GPS," *Global Positioning System: Theory and Applications*, Volume II, Cambridge, Massachusetts, 1996, pp. 397-425.

[9] Braff, R., Powell, J. D., and Dorfler, J., "Applications of GPS to Air Traffic Control," *Global Positioning System: Theory and Applications*, Volume II, Cambridge, Massachusetts, 1996, pp. 327-374.

[10] Bryson, A. E., *Control of Spacecraft and Aircraft*, Princeton University Press, Princeton, NJ, 1994.

[11] Kang, W., De, P. K., and Isidori, A., "Flight Control in a Windshear via Nonlinear H_∞ Methods," *Proceeding of the 31st Conference on Decision and Control*, Tucson, Arizons, December 1992, pp. 1135-1142.

[12] Skogestad, S., and Postlethwaite, I., *Multivariable Feedback Control Analysis and Design*, Wiley, New York, 1996.

[13] Magni, J. F., Bennani, S., and Terlouw, J., *Robust Flight Control: A Design Challenge*, Springer, London, 1997.

[14] Chen, D., and Paden, B., "Stable Inversion of Nonlinear Nonminimum Phase Systems," *Proceeding of Japan/USA Symposium on Flexible Automation*, 1992, pp. 791-797.